Nucleation of water vapor on the surface of a silver iodide crystal: Numerical experiment

S. V. Shevkunov

Saint Petersburg State Technical University, 195251 Saint Petersburg, Russia
(Submitted 11 January 1995)
Zh. Éksp. Teor. Fiz. **108**, 1373–1402 (October 1995)

The interaction of the surface of a silver iodide crystal with supersaturated vapor at $T=253$ K is modeled using the grand canonical ensemble Monte Carlo method. The intermolecular interactions are described by the modified five-center ST2 potential of Rahman and Stillinger. The water-lattice interaction includes explicitly non-pair polarization terms. The microstructure of the adsorbed phase is studied in detail. The surface of an ideal silver iodide crystal exhibits a moderate stimulating influence on the nucleation of vapor far from that observed under natural conditions for a real crystal. The unfavorable orientational order within the first monolayer hinders growth of the dense phase of water on the surface. The situation changes drastically after a certain supersaturation threshold is exceeded, and the Markov process transitions into the nonstationary regime corresponding to the thermodynamic instability. The growth of subsequent monolayers is accompanied by an abrupt reorientation of the electric dipole moments of the molecules in the first monolayer. The presence of lattice point defects qualitatively changes the nucleation regime, but also in this case the development of an instability leading to avalanche-like growth of a water dense-phase nucleus on the crystal surface takes place at the same high values of supersaturation as in the absence of any defects. The strong and highly localized electric field of the lattice point defect stabilizes the molecular cluster and interrupts its growth at 10–30 molecules, depending on the specific conditions and type of lattice defect. The microstructure of the dense-phase nucleus is far from that of ice. This is the main reason for retardation of its growth. The point defects on the surface of the crystal are not able to radically increase the activity of the silver iodide crystal as a stimulator of heterogeneous nucleation.

1. INTRODUCTION

Heterogeneous nucleation of water vapor on ions and ionic crystals is a key problem in the development of practical means of actively influencing atmospheric processes. Nucleation centers in supersaturated layers of the atmosphere are introduced by dispersing finely divided crystals, obtained by mechanical crushing and heat processing, from airborne platforms. The mass of the dispersed reagent is vanishingly small in comparison with the mass of moisture brought into motion. Significant amounts of heat are liberated in the nucleation process, altering the total temperature regime of the atmosphere and causing artificial convective displacements of air mass. The immediate result of this action can be local precipitation in the form of downpours or snowfall. This artificial local precipitation can be used to wash accidental emissions of either a chemical or a radioactive nature out of the atmosphere with the goal of localizing regions of pollution.

Experimental studies of the interaction of aerosols with atmospheric moisture have been pursued already for several decades;[1] however, there have been more questions regarding the mechanism of this interaction than answers. On the one hand, there is a large body of experimental material on the activity of various reagents, while on the other hand no reliable explanation of the causes of the high activity of some compounds and the low activity of others is available. Those explanations that are advanced are of a hypothetical nature. This hinders a purposeful search for active materials. The most active reagent known today, silver iodide (AgI), is an expensive material, and field experiments with this material require large capital investments and are correspondingly severely limited in scale. The high activity of this compound was discovered, as frequently happens in experimental studies, in a purely accidental fashion, and a reliable explanation for its high activity has yet to be found. An explanation of the high activity of finely divided silver iodide in its interaction with water vapor can be expected to be nontrivial, since macroscopic crystals of AgI are only poorly moistened when brought in contact with water and do not dissolve in water. To disperse finely divided silver iodide powder, it is suspended in acetone and this suspension is then ignited. The hexagonal symmetry of the β-AgI crystal may be as the simplest explanation of the high activity of silver iodide, i.e., it is the same symmetry as that of ice and close to the short-range order in water. However, such an explanation ignores the relatively poor wettability of macroscopic crystals of AgI. It is possible that a decisive role is played here by surface defects of the crystal, formed during the preparation of the finely divided material. A study of this problem requires a detailed microscopic approach.

A consistent statistical-mechanical description of real systems at the micromolecular level is, as a rule, a very complicated task and realizable in practice only if a number of simplifying assumptions, such as weakly nonideal behavior, homogeneity, weak interparticle correlations, the presence of

 1063-7761/95/100753-17$10.00

a small parameter, macroscopic quantities spatial symmetry, etc., are fulfilled. Near the gas-liquid phase transition points and especially in the vicinity of the critical point the radius of the interparticle correlations grows without limit, and the statistical behavior of the system becomes very complicated theoretically. This reality is expressed in the divergence of series in powers of the density,[2–6] and the growing complexity of the coupling between the many-particle and binary spatial correlations in the system does not allow us to close the infinite chain of integral equations for the correlation functions.[7] Thus, the problem becomes hopeless for traditional approaches. Not only is there no consistent general theory of phase transitions, but the construction of a purely analytic theory for each specific intermolecular potential presents insurmountable difficulties of a calculational nature. The task becomes still more complicated when we try to describe the kinetics of phase transitions, including nucleus formation and metastable states, when the dimensions of the dense-phase nucleus are comparable to the dimensions of the molecules themselves. In this case ideas from the classical theory of capillarity of homogeneous droplets with a well-defined phase boundary lose their meaning.[8–13] It is unclear how to treat the surface of such a microdroplet and what surface tension to assign to it.

Among investigators in this field there exists a certain suspiciousness about the correctness of applying Gibbsian statistical mechanics to bounded molecular systems. Usually in statistical theory one speaks of colossal molecular ensembles which permit one to take the thermodynamic limit $N\to\infty$. This has created the impression that Gibbsian statistical mechanics is valid only for such systems. However, a detailed analysis of the derivation of the Gibbsian equilibrium distribution shows[14] that for it to be exact, it is sufficient that two conditions be fulfilled: 1) the macrothermostat with which the system is in equilibrium must be macroscopic, and 2) direct interactions between the particles of the system and the particles of the thermostat in comparison with the intermolecular interactions inside the system must be vanishingly weak. If these two conditions are fulfilled, a small molecular system, e.g., a dense-phase nucleus in equilibrium with a gas, remains Gibbs-distributed irrespective of the number of particles in it. This, however, does not mean that smallness of the system does not leave its stamp on its behavior. Whereas in a macroscopic molecular system the relative statistical fluctuations of all the characteristics vanish, the distributions themselves acquire a δ-function-like character, in a small system the relative fluctuations are finite and the distribution functions have a finite half-width. The asymmetry of these distributions causes the mean values and the most likely values to differ. This difference is why different statistical ensembles for one and the same system are not equivalent.[15] This nonequivalence of ensembles is not a "defect" of the theory, but rather reflects the real dependence of the behavior of a small system on the specific boundary conditions. If we are to speak of thermodynamic quantities calculated for a small system, then, strictly speaking, it is necessary to indicate which statistical ensemble they pertain to. In the limit $N\to\infty$ the differences level out.

Phase transitions as mathematical singularities in the functional dependence of the free energy and its derivatives on the external thermodynamic variables—temperature, pressure, density, etc.—have meaning only in the thermodynamic limit $N\to\infty$. For finite values of N the zeros of the partition function of the grand canonical ensemble, associated with phase transitions, are located in the complex plane of values of the activity at finite distances from the real axis,[16] and among the physically admissible thermodynamic states there are no singular points; however, the nearness of the zeros to the real axis manifests itself in the relatively abrupt variation of the thermodynamic potentials of bounded molecular systems around these points on the real axis. In spite of the absence of singularities in the strict sense, it is customary to speak of microcondensation, evaporation, microcrystallization, and melting in small systems. Collective phenomena are quite distinctly manifested even in systems of several tens and just several molecules.[17–33] Phase transformation points of a small system can be greatly shifted relative to the phase transitions in the corresponding macroscopic systems. This shift depends strongly on the type of intermolecular interactions—the long-range force, orientational dependence, screening. For example, in a system of 16 argon atoms the droplet formation point is two times lower in temperature than in the macroscopic system, and the microcrystallization point, three times lower.[25,26] In an ionic system this shift is insignificant.[27–31] The shift of the melting point due to smallness of the system can also be observed under natural conditions.[32] The marked difference in the temperatures of microdroplet formation and condensation of the macroscopic bulk phase is the reason for the formation of metastable states—a supercooled (supersaturated) vapor. Since simultaneous condensation throughout the entire volume is unlikely, the gas–dense phase phase transition passes through a stage of random formation and growth of microdroplets (clusters). The smaller the size of the nucleus, the higher is the probability of its spontaneous formation, but that much lower should then be the temperature for its stabilization and growth in the gas. The critical size corresponds to unstable equilibrium of the nucleus with the gas at given temperature and density of the gas. Supersaturation (supercooling) of the gas leads to a decrease of the critical size down to values such that the probability of fluctuational formation of critical nuclei ensures a high rate of growth in the system, i.e., condensation takes place. The nucleation rate varies exponentially with variation of the external conditions. A nucleation rate on the order of 1 nucleus/cm^3 is commonly taken as the threshold value at which condensation of a supersaturated vapor takes place in times observable under natural conditions.

A critical nucleus corresponds to a maximum in the work of forming a microdroplet from the gas and places an obstacle in the path of homogeneous nucleation. This obstacle can be sharply lessened by introducing admixtures into the gas, i.e., nucleation centers. The shape of the functional dependence of the work of formation on the size of the clusters formed on the admixtures can have a very different shape and is determined by the nature of the interaction of the molecules of the vapor with the particles of the admixture. The particles of the admixture should not just represent

a potential well—the structure of the attractive field of the nucleation centers should be such that the water molecules pulled into this field are arranged in an order near to the molecular order in the macroscopic dense phase. If they are not, then growth of the nucleus stops at a size whose stability is the outcome only of direct interactions with the admixture particles—further growth due to attractive collective interactions between the molecules is impossible. As I showed in one of my previous papers,[33] it is just this type of situation that can take place during nucleation to free ions of Ag^+ and I^-. The structure of the nascent dense phase turns out to be "crushed" in the strong electric field of the ions. The molecular order imposed by the ions is far from the close-range molecular order in an ice crystal or in water, and a calculation of the number of molecules in the first few coordination layers shows that this order is closer to cubic than to hexagonal symmetry. Therefore growth of the nucleus stops as early as the formation of the second molecular layer around the ion; only in the presence of strong supersaturation, hardly attainable under real conditions, does a third layer take shape. It is not possible to stabilize the third layer as the result of direct interactions with the ions, but the configuration in which the molecules of the first and second layers find themselves turns out to be noncomplimentary to the structure of the stable liquid phase in the third and subsequent layers, so growth of the nucleus ceases and very stable cluster ions are formed, containing from several up to around 20 water molecules, depending on the humidity and temperature. The probability of recombination of such hydrated ions, obviously, is sharply decreased relative to the free ions, which may favor their accumulation.

Analogous studies in the interionic interval of Ag^+I^- (Ref. 34) lead to a qualitatively similar picture, although the symmetry of the arrangement of the molecules in the field here is different, and, depending on the interionic distance, the binding energy exhibits a complicated, irregular behavior. In the axially symmetric distribution of the density of the nucleus, a cavity is formed around the axis joining the ion centers. As a whole, the molecular order imposed by the strong electric field of the ions is far from that in the condensed phase of water, and growth of the nucleus comes to a halt even in the presence of strong supersaturation.

2. METHOD

In the calculations presented here the intermolecular interaction is described by the five-point pairwise potential ST2 of Rahman and Stillinger.[35–37] The Hamiltonian of the system explicitly includes the Coulomb, exchange, and dispersion interactions between the water molecules and, implicitly, the polarization interaction. In the interaction of a water molecule with ions of the AgI crystalline lattice Coulomb, dispersion, exchange, and nonpairwise polarization terms are explicitly present, and polarization of the molecules in the field of the ions as well as polarization of the ions in the field of the water molecules is taken into account. The latter is due to the relatively strong electric field of the ions and their high polarization coefficients. The chemical bonds in the AgI crystal are not purely ionic. Partial overlap of the electronic shells, as in Ref. 38, is also taken into account: the Ag^+ ion is assigned the charge $+0.6e$, and the I^- ion the charge $-0.6e$, where e is the elementary charge. The Hamiltonian of the system is described in my earlier paper,[33] to which the reader is referred for details, and in the present section we will concentrate on the calculational algorithm.

Numerical modeling is the only method that will work when the approximate methods of statistical mechanics will not. Numerical modeling techniques are traditionally divided into two groups: equilibrium and dynamic. The first includes the Monte Carlo method (the Metropolis method) in its original formulation.[39,40] The second includes the molecular dynamics method[41] and special combined approaches, e.g., the Brownian dynamics method,[42–44] the dynamic Monte Carlo method,[45,46] and the isothermal molecular dynamics method.[47] While the Monte Carlo method and the molecular dynamics method are, in essence, exact methods, their combinations represent efforts to construct some approximate means of calculating by classifying molecular motion according to a temporal hierarchy. There are special exact modifications of the Monte Carlo method, aimed at a direct calculation of the free energy.[48] The present paper makes use of only the Monte Carlo method in its exact formulation.

The Monte Carlo method is based on fundamental results of Gibbsian statistical mechanics and does not require any approximations: for a given model intermolecular potential the problem is, in principle, exactly solvable; the only limitation on the accuracy of the results is the finite size of the statistics in the calculation of the equilibrium mean values. The statistical error is decreased by simply extending the sequence of molecular configurations included in the statistics. The Monte Carlo method consists in averaging over a configurational subspace of the system, wherein the mechanical momenta of the molecules are excluded from the averaging process. Such a reduction of the number of variables does not imply any approximation, rather it is based on the well-known property of the partition function of a classical system: the integral over states decomposes into a product of an integral over the coordinates and an integral over the momenta of the molecules, whereby the integration over the momenta can always be accomplished analytically and reduces to a well-known trivial result.[16] Thus, the problem of calculating the integral over states and the equilibrium mean values reduces to an integration over molecular configurations, which in fact is what is realized by the Monte Carlo method. The Monte Carlo method reduces to the generation, with the help of a high-speed computer, of a sequence of from hundreds of thousands to tens of millions of molecular configurations in such a way that the frequency of occurrence of a configuration is proportional to the Gibbs equilibrium distribution function $\exp(-U_N(q_1,\ldots,q_N)/kT)$, where $U_N(q_1,\ldots,q_N)/kT$ is the potential energy of the interaction of the molecules in the system, $x \equiv q_1,\ldots,q_N$ are the coordinates of all the molecules in the system (a point in $6N$-dimensional configuration space), k is the Boltzmann constant, and T is the absolute temperature. The order of appearance of the configurations does not necessarily coincide with their order of appearance following from the dynamical equations controlling the evolution of the system in real time, but this is not required, since the goal consists in

calculating the equilibrium mean values, and the values of the accumulating sums do not depend on the order of terms in these sums. Permuting the terms in the sums allows one to economize on the volume of calculations by orders of magnitude. The price for this is a loss of information about the dynamics of the evolution of the system in real time, i.e., the impossibility of studying nonequilibrium states.

The molecular configurations are obtained with the help of a Markov random walk process in the configuration space of the system.[49] The uniform Markov random process in continuous state space is directed by the density function of the probabilities $p(x,y)$ of the transition $x \to y$. The kth step of the process consists in reassigning the distribution function $\rho^k(x)$ over the ensemble of states according to the governing equation

$$\rho^k(y) = \int \rho^{k-1}(x) p(x,y) dx. \tag{1}$$

If the ergodicity conditions for the kernel function $p(x,y)$ are fulfilled,[49] then the stability theorem applies, according to which the process (1) reduces to the single limiting distribution

$$\lim_{k \to \infty} \rho^k(x) \to \rho(x),$$

which satisfies the equation

$$\rho(y) = \int \rho(x) p(x,y) dx. \tag{2}$$

In the Monte Carlo method, Eq. (2) is taken as the condition for the kernel function $p(x,y)$ for a prescribed Gibbs limiting distribution

$$\rho(x) \propto \exp(-U_N(x)/kT).$$

Equation (2) does not determine the transition probabilities $p(x,y)$ uniquely. The remaining degrees of freedom in determining $p(x,y)$ are used to construct the most economical and fastest-converging (to the limiting distribution) process. In addition to condition (2), the transition probabilities usually obey the stronger condition of detailed balance

$$\rho(y) p(y,x) = \rho(x) p(x,y). \tag{3}$$

Condition (2) follows from condition (3) by integrating over x, taking into account the normalization condition $\int p(y,x) dx = 1$. Condition (3) also does not determine $p(x,y)$ uniquely.

The numerical implementation of the Markov random process in fact tracks one representative of the ensemble of parallel-evolving systems, and the ensemble average is replaced after reaching the limiting distribution by the average over the Markov steps for one system. In the calculational algorithm used in the present work, one Markov step consists in a translation and rotation of one randomly chosen molecule, or the insertion into the system of one molecule with placement at some randomly chosen point in space, or the removal of one randomly chosen molecule from the system. The latter two types of steps are performed five times as often as the first, and the ratio of the frequency of the first type of step to that of the third type is 1:1. The probabilities of these different acts are assigned with the help of a random number generator, i.e., a special subprogram, returning uncorrelated random numbers ξ, uniformly distributed over the interval (0,1) each time it is called . At the translation step, with the help of the random number generator, the number n of the molecule to be translated is assigned. Next, the displacement vector of the center of mass of the molecule, with components $\Delta x, \Delta y, \Delta z$ is randomly assigned with equal probability from the fixed interval $(-\delta, +\delta)$ and the increment in the Euler angles $\Delta\alpha$, $\Delta\vartheta$, $\Delta\varphi$ is randomly assigned with equal probability from the fixed interval $(-\varepsilon, +\varepsilon)$. Next, the change in the interaction energy in the system due to the translation $q_n \to q_n'$ is calculated:

$$\Delta U = U_N(q_1, \ldots, q_{n'}, \ldots, q_N) - U_N(q_1, \ldots, q_n, \ldots, q_N),$$

and the inequality

$$\exp(-\Delta U/kT)\ \sin(\vartheta + \Delta\vartheta) > \xi\ \sin\vartheta, \tag{4}$$

is checked in which the random number ξ participates. If inequality (4) is satisfied, then the nth molecule is moved to the new point with coordinates $q_{n'}$. If not, then it stays where it is, at q_n. Either way, this completes the step. It is not hard to verify that such an algorithm, irrespective of the specific values of the parameters δ and ε, corresponds to the transition probabilities obeying condition (3), with the limiting distribution function

$$\rho(x) \propto \exp\left(-\frac{U_N(x)}{kT}\right) \prod_{k=1}^{N} \sin\vartheta_k,$$

where ϑ_k is the Euler angle between the axis of the kth molecule and the z axis of the Cartesian coordinate system, and the product of sines in the distribution function is the Jacobian of the transformation to spherical coordinates.

Insertion and removal of molecules are performed analogously, with the one difference that instead of condition (4), in the case of insertion of a molecule, one tests the condition

$$\left(\frac{V}{V_0}\right) \exp\left(\frac{\mu_c - u_{N+1}}{kT}\right)\ \sin\vartheta > \xi, \tag{5}$$

where u_{N+1} is the potential energy of the inserted molecule and ϑ is its Euler angle,

$$\mu_c = \mu - kT\ \ln\left(\frac{\Lambda_{\rm tr}^3 \Lambda_{\rm rot}}{8\pi^2 V_0}\right)$$

is the configuration part of the chemical potential μ, $\Lambda_{\rm tr} = h/\sqrt{2\pi m kT}$ is the thermal De Broglie wavelength, h is Planck's constant, m is the mass of the molecule, $\Lambda_{\rm rot}$ is the result of integrating over all the angular momenta of one molecule in the partition function of the system, V_0 is an arbitrary fixed volume prescribing the reference level of μ_c, and V is the volume of the system. An attempt to remove a molecule reduces to an equiprobable choice of the number n—the candidate for removal from the system. The step is completed by striking one molecule from the list if

$$\left(\frac{V_0}{V}\right)\ \exp\left(-\frac{\mu_c + u_n}{kT}\right) > \xi, \tag{6}$$

where u_n is the potential energy of the molecule to be removed. It is not hard to convince oneself that although the condition of detailed balance (3) is violated in such an algorithm due to the inevitable overcounting in the list of molecules after the removal step, the main requirement (2) is fulfilled with the limiting distribution being that of the grand canonical ensemble[16]

$$\rho(x)d^NVd^N\Omega \sim \frac{1}{N!}\exp(\mu_c N/kT)\exp(-U_N/kT)$$
$$\times \frac{d^NV}{V_0^N}\frac{d^N\Omega}{(8\pi^2)^N} = \frac{1}{N!}\frac{1}{\Lambda_{\rm tr}^{3N}}\frac{1}{\Lambda_{\rm rot}^N}$$
$$\times \exp(\mu N/kT)\exp(-U_N/kT)$$
$$\times d^NVd^N\Omega, \qquad (7)$$

where the factor $1/N!$ in Eq. (7) enters when the molecule number at the removal step is played and the last number in the list is indicated at the insertion step; the remaining factors in Eq. (7) come from the transition probabilities with the choice of a specific position and orientation of the molecule inserted in the volume V.

Although the mass of the molecules enters into formulas (5) and (6) formally via μ_c and $\Lambda_{\rm th}$, and the principal moments of inertia of the molecule enter through $\Lambda_{\rm rot}$, in actual fact the transition probabilities do not depend on the mass or on the moments of inertia and are determined only by the intermolecular interactions. This is because the chemical potential μ contains the term $\ln(\Lambda_{\rm tr}^3\cdot\Lambda_{\rm rot})$, which is compensated by the corresponding term in the expression for μ_c in terms of μ, as a result of which there is no dependence on $\Lambda_{\rm tr}$ or $\Lambda_{\rm rot}$ in μ_c. Performing the elementary transformations using the well-known thermodynamic relations, it is easy to show that in the case of an ideal gas

$$\mu_c = kT\ \ln\frac{PV_0}{kT}, \qquad (8)$$

where P is the gas pressure. According to relation (8) the transition probabilities are in fact determined by the water vapor partial pressure. Our calculations, carried out to compare the chemical potential of the molecules of water vapor and the water vapor partial pressure in the atmosphere, use the ideal gas approximation (8), and our numerical results are presented in terms of partial pressures—converting back to the chemical potentials can be done with the help of relation (8) and the relation between μ_c and μ.

3. BOUNDARY CONDITIONS

The condensed-phase nucleus forming on the surface of the silver iodide crystal finds itself, on the one hand, in thermal and material contact with the water vapor above the surface of the crystal and, on the other hand, in the force field of the ions of the surface layers of the AgI crystalline lattice. The configuration of this field depends on the structure of the lattice and the crystallographic face along which the cleavage sheet is split off. Three stable modifications of silver iodide are known, differing in the symmetry of the crystalline lattice:[50,51] the α modification is body-centered cubic, the β modification is hexagonal, and the γ modification is face-centered cubic. α-AgI is stable at temperatures above 147 °C, and γ-AgI is the metastable phase. The modification β-AgI is absolutely stable under atmospheric conditions. The symmetry of the β-AgI lattice belongs to the hexagonal system with spatial group $P6_3mc$ (Ref. 52). The unit cell of the β-AgI lattice is base-centered and possesses a mirror symmetry plane, Fig. 1. The lattice constants at zero temperature are: $a=4.580$ Å, $c=7.494$ Å (Ref. 53). Finite temperatures are reflected in the third significant digit in the lattice constants. According to neutron diffraction data,[51] at a temperature 80 K $a=4.592$ Å, $c=7.512$ Å, and at a temperature of 295 K $a=4.593$ Å, $c=7.510$ Å. This difference lies beyond the limiting accuracy of our calculations. Therefore, oscillations of the ions in the crystalline lattice are not taken into account, and the ions are taken to be rigidly fixed in their positions corresponding to absolute zero temperature.

In fact, the lattice of the β-AgI crystal consists of two hexagonal sublattices of Ag^+ and I^- ions, intermeshed, one in the other. The Ag^+ sublattice is displaced relative to the I^- sublattice along the rotational symmetry axis of the unit cell by 2.810 Å, which is less than the half-height of the cell $c/2=3.747$ Å by 0.937 Å, wherefore the layers of Ag^+ and I^- ions parallel to the bases of the unit cell are arranged pairwise: the distance in a pair between nearest layers of opposite ions is 0.937 Å, while the distance between pairs of layers is roughly three times larger, 2.810 Å. The pairs of layers in which Ag^+ ions are located above I^- ions alternate with pairs of layers in which the arrangement of the ions is the opposite. When the crystal is cleaved in a plane parallel to the bases of the unit cell, as one might expect, the mechanical strength of the bond between the layers 2.810 Å apart is less than that between the layers 0.937 Å apart, and on the cleavage surface one finds a pair of layers separated by 0.937 Å, with ions of one sign forming the surface itself.

When the crystal is cleaved parallel to a lateral face of the unit cell (Fig. 1) one finds ions of both signs on the cleavage surface (Fig. 2), and, in contrast to cleavages parallel to the bases (Fig. 3), indications of hexagonal symmetry on the cleavage surface are absent. Ions of one sign on a lateral cleavage surface are arranged in straight lines parallel to the bases of the unit cell; lines with oppositely charged ions alternate (Fig. 2). The layers parallel to the lateral faces of the unit cell are all the same distance apart (1.322 Å) and are offset, one from the other, by $a/2$ and $c/2$ along the corresponding edges of the unit cell.

Comparison of the microstructure of the cleavages parallel to the bases and the lateral faces of the unit cell of β-AgI leads to the following conclusions. On a cleavage parallel to a base, the electric field of the ions is more uniform than on a cleavage parallel to a lateral face. Numerical calculations show[38] that the diffusion barrier for molecules of H_2O on the basal faces is 2.5 kcal, while on the lateral faces it is 8 kcal. The largest binding energy of a water molecule with the surface of the crystal is found on a lateral face and is 19.9 kcal, and the corresponding potential well is very narrow. About the same binding energy (19.4 kcal) is found on faces parallel to a base, near a defect formed by removal of an I^- ion, at three neighboring points separated by 0.25 Å.

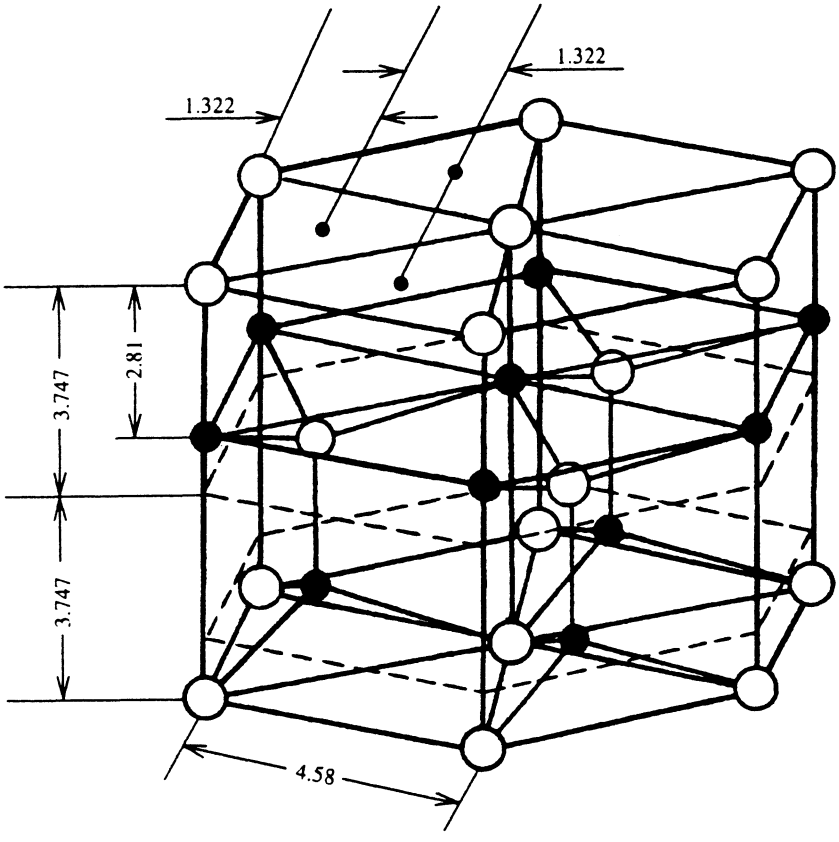

FIG. 1. Unit cell of the crystalline lattice of β-AgI. Filled circles depict the equilibrium positions of the Ag^+ ions, empty circles depict the I^- ions. All distances in Ångstroms.

If adsorbed water molecules are positioned at the points of minimum energy on the surface of a cleavage parallel to the bases of the unit cell, without allowing for interactions between the molecules, a monomolecular layer is formed with

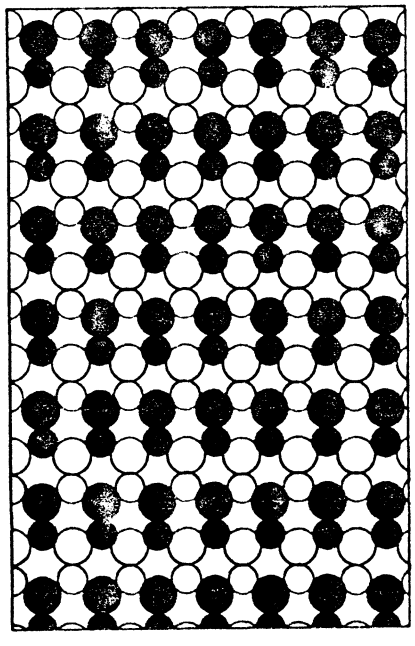

FIG. 2. Positions of the ions in the β-AgI lattice in the first two layers of a cleavage sheet of the crystal parallel to a lateral face of the unit cell. The filled circles depict the positions of the Ag^+ and I^- ions in the first (surface) layer, and the empty circles depict the ions in the second layer. The large circles are the I^- ions, and the smaller circles are the Ag^+ ions. The distance between the first and second layers is 1.322 Å. The third crystalline layer (not depicted in the figure) is located 2.644 Å below the second.

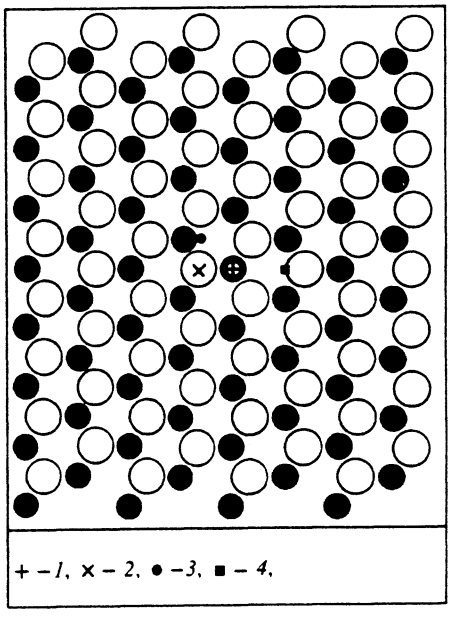

FIG. 3. Positions of the ions in the β-AgI lattice in the first two layers of a cleavage sheet of the crystal parallel to the bases of the unit cell. The filled circles depict the positions of the ions in the first layer, and the empty circles depict the ions in the second. All the ions of the first layer are Ag^+ ions, and all the ions of the second layer are I^- ions. The distance between the first and second layers is 0.937 Å. The third crystalline layer (not depicted in the figure) is located 2.810 Å below the second marks indicate the points are marked, above which the local density distributions in height above the crystal surface were calculated.

hexagonal symmetry. In the resulting structure the positions of the centers of mass of the water molecules are very close to the positions of water molecules on the surface layer of ice; however, the position of the hydrogen atoms of the molecules turns out to be unfavorable for the formation of the ice structure.

In the present paper we study nucleation on the faces parallel to the bases of the unit cell of AgI—the basal faces. Although the basal faces have points with maximum binding energy, the geometry of the arrangement of these points does not possess hexagonal symmetry and is far from the structure of ice and of liquid water. The relatively high diffusion barriers on the lateral faces make the microstructure of the first monomolecular water layer on the surface of the crystal more rigid, leaving less of a possibility for relaxation to the independently stable dense-phase structure of H_2O. This does not mean that we are discarding beforehand the possibility of favorable conditions for nucleation on the lateral faces, much less in a crystalline lattice with defects; however, the bases of the unit cell present themselves to us as more likely candidates for the role of a complimentary substrate for dense-phase H_2O.

The interaction of each water molecule with the AgI lattice at each step of the Monte Carlo procedure is computed by directly summing the interactions with each ion in the lattice, so the number of ions that it is actually possible to take into account in the calculations is determined by the speed of the computer and is usually not more than a few hundred in the layers near the surface. Long-range interactions can be taken into account by the Ewald method,[54] which is to sum the electric fields of the infinite periodic lattice in the conjugate Fourier space (sum over the inverse lattice). It is of fundamental interest to elucidate the relative role of the surface ions and the deep ions of the crystalline lattice in initiating nucleation. Therefore it would be advantageous to gradually increase the number of layers taken into account in the calculations. Following this logic, we begin our numerical experiments with two layers a distance of 0.9368 Å apart with hexagonal symmetry of the ions as in the bases of the AgI unit cell. The surface (first) layer contains only Ag^+ ions, the second layer—only I^- ions. The second layer is displaced in its own plane along the mutually perpendicular directions of translational symmetry by $\Delta x = 2.644$ Å and $\Delta y = 2.290$ Å, so that the I^- ions are located as in a real AgI lattice at equal distances (2.81 Å) from the three nearest Ag^+ ions in the first layer (see Fig. 3). In a real AgI lattice the distance to the next (third) layer is also 2.81 Å, so each I^- ion is surrounded by four nearest Ag^+ ions at equal distances of 2.81 Å lying on the rays of a tetrahedron, and, conversely, each Ag^+ ion lies at the center of a tetrahedron formed from I^- ions (see Fig. 4). The edge of the tetrahedron is 4.58 Å in length.

Layer fragments consisting of $8\times8=64$ Ag^+ ions and the same number of I^- ions, altogether 128 ions, are modeled. The surface fragment has dimensions 28 Å×32 Å. About 100 water molecules would be arranged in a monomolecular layer on such a fragment. Above the crystal surface the open ensemble method is used to model an equilibrium vapor of water molecules, which is allowed the possibility of freely depositing or evaporating from the surface of the crystal in accordance with the exact Gibbs distribution over microstates. Although under real conditions the vapor is a molecular ensemble of macroscopic dimensions, it is meaningful to allow for the direct interaction of the surface with molecules not further away than a few Ångstroms since the interaction potential falls off rapidly with distance. In the experiments which we will present, only the direct interaction with molecules inside a hemisphere with radius $R_0=10$ Å above the surface of the crystal is taken into account. The center of the hemisphere lies at the center of the fragment in the plane of the first crystal layer. Thus, roughly a third of the area of the (28 Å×32 Å) fragment lies under the hemisphere; the remaining ions of the fragment lie outside the limits of the hemisphere and are needed to smooth out nonphysical boundary effects on the boundary of the sphere. The volume of the hemisphere is large enough to accommodate roughly 70 water molecules under it in the liquid phase, so the size of the nucleus approaching this value in the numerical experiment would mean that removing the limiting sphere would lead to further growth of the nucleus.

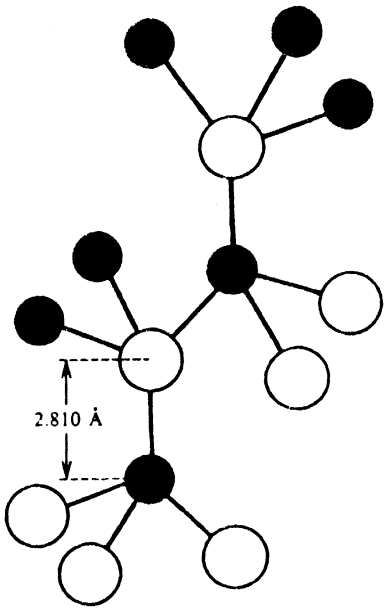

FIG. 4. Spatial fragment of the crystalline lattice of β-AgI with tetrahedral structure of the interionic bonds between oppositely charged ions.

Since there are no third or deeper layers in the numerical experiments, it is necessary to forbid the adhering of water molecules below the second layer. In our calculations, those states are forbidden in which the water molecules penetrate into the crystal beyond a prescribed depth $h_{min}=-3$ Å, measured from the plane of the first layer. Varying h_{min} allows us to examine the penetration depth of the water molecules in a real crystal and its role in the formation of the dense phase on the surface. In this regard, it should be noted that modeling nucleation on individual Ag^+ and I^- ions[33] shows that the distance of closest approach between an ion and a water molecule (the oxygen atom of the molecule) is approximately 2 Å, and the first hydration layer is located at a distance of about 3 Å from the center of the ion. If we take into account that the lattice constant in the plane of the layer is

4.58 Å, there remains a channel roughly 0.5 Å in width for penetration of water molecules into the crystal. Varying the lattice constant can "close up" or "slightly open up" this channel.

4. NUMERICAL EXPERIMENTS

The first question we hope to answer in our experiments pertains to the thermodynamic stability of the water nucleus on the surface of the crystal. Two fundamentally different situations are theoretically possible. In the first case the Gibbs free energy $G(N)$ of the nucleus consisting of N particles, being nonlinear in the number of particles, is a convex function of N. In this case the work of forming the nucleus $A(N) = G(N) - \mu N$ for appropriate values of the chemical potential of the vapor μ passes through a maximum, and the position of the maximum N_c is the critical size, corresponding to unstable equilibrium with the vapor. The nucleation mechanism in this case does not qualitatively differ from that of homogeneous nucleation although the critical size can, all other conditions being equal, be less, and the nucleation barrier lower. In the second case the dependence $G(N)$ is concave, and $A(N)$ passes through a minimum at a value N_s corresponding to a thermodynamically stable size of the nucleus. Under such conditions, stable molecular clusters are formed on the surface of the crystal. The second situation is possible only within a range of sufficiently small N since for large N, when equilibrium of the microdroplets enters into the regime of the classical theory of capillarity with positive surface tension, the function $G(N)$ necessarily becomes concave, and equilibrium of the droplet with the vapor is unstable. Stability of the nuclei means that their containing more than N_s particles is thermodynamically unfavored, in particular, due to coalescence with neighboring nuclei on the surface. Such a situation of unfavored growth can take place when the microstructure of the nucleus differs strongly from that of the stable bulk dense phase, i.e., due to a strong interaction with the surface of the crystal attaching to its structure. Thus, the stability of the microdroplet can be secured only by strong interactions with the microscopically inhomogeneous surface of the crystal. Microscopic inhomogeneity is enhanced by introducing crystalline defects.

All of the calculations presented in this paper were carried out for the temperature $T=253$ K. Saturated vapor pressure above a planar phase boundary for this temperature is 1.04 mbar (Ref. 55). The results presented in Fig. 5 correspond to both saturated and supersaturated vapor. The curves in Fig. 5 depict the variation of the local density of the water molecules as a function of the height h measured from the surface of the crystal above the centers of the Ag^+ and I^- ions in the first two layers of the crystalline lattice, i.e., above points *1* and *2* in Fig. 3. In the calculation of the local density we directly average the number of molecules whose centers of mass fall within the microvolume with dimensions 1 $Å^3$. To decrease the statistical error of the local density, we averaged over several ions in the central part of Fig. 3. In parallel, we calculated the distributions of the local water density above the points located between neighboring Ag^+ ions and between neighboring I^- ions—points *3* and *4* in Fig. 3, respectively. The local densities above these points

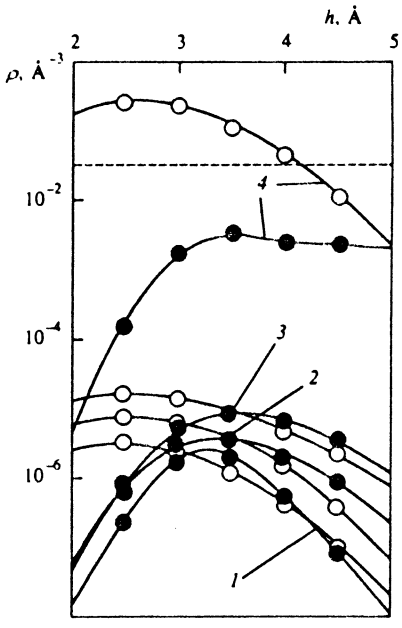

FIG. 5. Local density distributions of water molecules above various points above the surface of a β-AgI crystal without defects at $T=253$ K: above the I^- ions (empty circles) and above the Ag^+ ions (filled circles). Here and in the following figures the surface of the cleavage sheet is parallel to the bases of the unit cell. Vapor pressure above the crystal: *1*) $P=1$ mbar, *2*) $P=3$ mbar, *3*) $P=9$ mbar, *4*) $P=27$ mbar. Dashed line—bulk water density under normal conditions.

were found to be two orders of magnitude less than above points *1* and *2* and are not shown in Fig. 5. A strong nonuniformity in the local power of the crystalline surface to adsorb water molecules is observed. The preferred segments of deposition of water molecules are the regions above the centers of both the Ag^+ and the I^- ions. The maximum of the local density above the Ag^+ ions is reached at a height of 3.3–3.7 Å above the surface, and the maximum above the I^- ions, at a height of 2.5 Å. Since the layer of I^- ions lies 0.937 Å below the layer of Ag^+ ions, the maxima are attained at roughly the same distance from the corresponding layer—3.5 Å. As the vapor pressure increases from 1 to 9 mbar, the maximum above the Ag^+ ions shifts from 3.3 to 3.7 Å, whereas the position of the maximum above the I^- ions remains unchanged (see Fig. 5). According to the results of my previous numerical experiments on the formation of a hydration coat of isolated ions,[33] the first hydration layer of the Ag^+ ion is located at a distance of 2.9 Å from the ion, and its position is stable with respect to variation of the vapor pressure. Its stability is explained by the formation of a specific structure with cubic symmetry. Displacement of the first hydration layer above the surface of the crystal by a distance of from 0.5 to 0.8 Å is explained by collective effects underlying the stability of the dense phase at larger distances from the ions; however, the stabilization effect is very weak, and at distances greater than 5 Å the density approaches values that are more characteristic of the homogeneous gas phase ($3\cdot10^{-8}$ $Å^{-3}$ for $P=1$ mbar (see Fig. 5).

There is an uncertainty in the position of the boundary of the adsorbed layer of water molecules of the order of 0.2 Å, associated with the natural thickness of the transition layer. To within this uncertainty the results of our numerical ex-

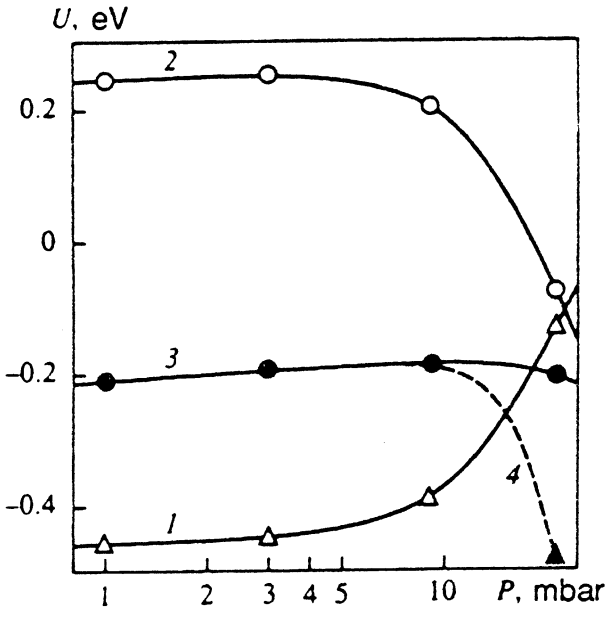

FIG. 6. Statistical mean interaction energy of the molecules of the nucleus in the calculation per molecule at $T=253$ K: *1*—interaction with the Ag^+ ions, *2*—interaction with the I^- ions, *3*—total interaction with all the ions of the β-AgI crystalline lattice, *4*—total interaction energy of the water molecules with the crystal surface and the remaining molecules of the nucleus. Crystalline surface without defects.

periments make it possible to estimate the thickness of the adsorbed layer at 5.0 Å for $P=1$ mbar, 5.2 Å for $P=3$ mbar, and 5.5 Å for $P=9$ mbar. The distribution of adsorbed molecules with height, measured from the surface of the crystal, varies greatly. At distances greater than 3.5 Å from the surface the densities above the Ag^+ and I^- ions practically coincide. At distances near 3.5 Å the difference in the local densities above the silver and iodine ions reaches 1–1.5 orders of magnitude (Fig. 5). The height of 2.6 Å above the surface of the crystal above the center of an I^- ion (above point 2, Fig. 3) turns out to be the most favorable for the water molecules. In this case the molecule finds itself in the potential well of the field of the three nearest Ag^+ ions and the weaker field of opposite sign of the I^- ion located directly under the molecule. The total electric field at this point points up from the surface of the crystal, as does the dipole moment of the molecule drawn into this field. This orientation of the molecule is confirmed by the positive sign of the mean energy of the interaction with the negative I^- ion (Fig. 6). The molecules located above an Ag^+ ion are also oriented upward by their dipole moments from the surface of the crystal. As for the positions above the nodes of hexagonal symmetry, unfilled by either ions of the first or ions of deeper layers of the lattice, the field above these points vanishes from symmetry considerations. Thus, the electric field of the lattice at the points above the surface of the crystal that are the most favorable for the molecules imposes the same orientation of their dipole moments as hinders the formation of a second monomolecular layer and the growth of dense phase above the surface of the crystal. A compensating external electric field, perpendicular to the plane of the crystal, would facilitate the reorientation of some of the adsorbed molecules and, possibly, stimulate the growth of the condensed phase.

The mean bulk density of the water molecules in the layer between the plane of the surface of the crystal (the plane of the centers of the Ag^+ ions) and the outer boundary of the layer is $n_v=2.1\cdot10^{-5}$ Å^{-3} for $P=1$ mbar, $3.2\cdot10^{-5}$ Å^{-3} for $P=3$ mbar, and $5.0\cdot10^{-5}$ Å^{-3} for $P=9$ mbar, i.e., $1.6\cdot10^3$, $1.0\cdot10^3$, and $0.6\cdot10^3$ times smaller than the bulk density of water under normal conditions. The difference of the density of the adsorbed phase by three orders of magnitude from that of liquid water does not leave any hope for the possibility of the development in this system of collective interactions similar to the interactions in the bulk phase of water, capable of stabilizing the nascent dense phase and ensuring its growth. In the numerical experiment one does not observe growth of the thickness of the adsorbed molecular layer beyond the values given above all the way to supersaturation of the vapor by one order of magnitude.

The state of the adsorbed phase on the surface of the crystal is characterized as extraordinarily loose. Collective binding interactions between the particles drawn into the field of the neighboring ions are practically absent. Such a picture is also confirmed by the character of the behavior of the binding energy of the water molecules with the Ag^+ and I^- ions and between the molecules themselves (see Fig. 6). All the way to pressures of $P=10$ mbar the contribution to the energy of the adsorbed layer from the intermolecular interactions is vanishingly small. The absence of a noticeable interaction between the molecules is explained by the extraordinarily low density of the adsorbed phase: at such a density the probability of finding two water molecules simultaneously at the surface of the crystal at a distance equal to the radius of the intermolecular interactions is close to zero. Stabilization of the adsorbed phase is ensured only by direct interactions with the ions of the lattice, whereby the interaction with the Ag^+ ions has a stabilizing character (negative energy), and the interaction with the I^- ions, a loosening character (positive energy); the total energy is negative and equal roughly to $-9kT$.

Figure 7 plots the surface density n_s of the adsorbed water molecules on a basal face of a silver iodide crystal as a function of the density of the supersaturated vapor. Growth of n_s is ensured mainly by condensation of the adsorbed layer and is approximately incorporated in the dependence $n_s \propto \sqrt{P}$. The deviation from a linear dependence on the side of slowing down suggests that the nascent collective intermolecular interactions at this stage do not stimulate, on the contrary they slow down the formation of the condensed phase—the most suitable vacancies near the surface of the crystal become filled with growth of the vapor pressure, while formation of new vacancies is possible only after an appropriate reorientation of the already adsorbed molecules. In turn, rotation of the water molecules is held up as a result of their large dipole moments interacting with the crystal field. Thus, the relatively large dipole moment of the water molecule, on the one hand, exerts a positive effect on adsorption, ensuring a strong interaction of the first monomolecular layer with the crystal and, on the other hand, this same dipole moment is the reason for the loosening interactions between

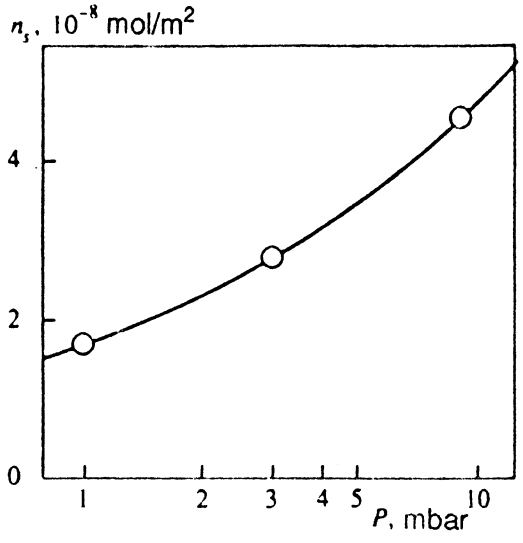

FIG. 7. Surface density of the adsorbed water molecules on a base face of a β-AgI crystal without defects in a supersaturated atmosphere at $T=253$ K.

the molecules, since their dipole moments acquire a preferentially parallel orientation and repel each other. The energy of the dipole–dipole repulsion is of the order of kT at a distance of roughly 6 Å. Within the range of these forces about the adsorbed molecule there turn out to be six nearest positions above ions of either sign, and six above ions of the other sign, vacant for capture of molecules from the vapor. These vacant points are practically "out of play" for an already captured molecule. The dipole–dipole repulsion has the result that not all of the surface of the crystal plays a part in the adsorption process, rather only 3 – 5 % of it, and the collective binding interactions in the ensemble of molecules are blocked.

Simple estimates show that such an adsorptivity is not capable of providing noticeable absorption of moisture from the atmosphere. In fact, the number of water molecules adsorbed by M spherical aerosol particles of radius r is equal to $N=M\cdot 4\pi r^2 n_s$. This amount of water is contained in a volume

$$V_{\text{vap}}=NkT/p=M\cdot 4\pi r^2 n_s kT/P$$

of the atmosphere. In turn, to obtain M aerosol particles requires an amount of silver iodide by volume equal to

$$V_{\text{cryst}}=(4/3)\pi r^3 M.$$

The efficiency of the aerosol is estimated by the ratio

$$V_{\text{vap}}/V_{\text{cryst}}=3n_s kT/Pr. \qquad (9)$$

Substituting the numerical values $P=1$ mbar$=10^2$ Pa, $r=10^{-6}$ m, $n_s=1.7\cdot 10^{-8}$ mol/m$^{-2}=1.0\cdot 10^{16}$ m^{-2} (Fig. 7) into Eq. (9), we obtain $V_{\text{vap}}/V_{\text{cryst}}=1.1$. In other words, to bind the moisture in 1.1 m^3 of saturated air would require 1 m^3 of crystalline material. The efficiency (9) can be increased by increasing the fineness of the aerosol, i.e., by decreasing r; however, micron-sized particles lie at the limit of what is technically attainable, and the efficiency (9) differs from what is meaningful in practice by orders of magnitude.

Thus, simple adsorption on the surface of an ideal AgI crystal is not capable of providing an effective mechanism for absorption of moisture from the atmosphere—the key factor here is the appearance of an instability in the equilibrium with the vapor. We were able to obtain such an instability, but only with extreme supersaturation. At $P=27$ mbar, a qualitative change in the deposition regime of water molecules on the surface of an ideal silver iodide crystal is observed. The Markov process was begun with one molecule in the system. Over tens of thousands of steps the number of molecules oscillated between zero and unity, rarely exceeding two, but then it abruptly broke away to larger values and began to grow in an avalanche-like fashion until all of the volume under the bounding hemisphere of radius 10 Å was filled with molecules. At this point the growth stops. Obviously, if one were to take away the bounding hemisphere, the growth would continue and the microdroplet would reach macroscopic dimensions. There is no doubt that we are dealing here with a situation in which, as a result of strong supersaturation, the critical size of the microdroplet on the surface of an ideal crystal has decreased to a few molecules and has become reachable in the process of random fluctuations of the size on the initial segment of the Markov trajectory. As a result of one of such "successful" fluctuations the size of the microdroplet passed through its critical value, ensuring its continued growth with lowering of the free energy of the system. We also reproduced such unstable behavior at higher levels of supersaturation. The higher the supersaturation, the shorter, on the average, the Markov "time" the system must spend before it achieves avalanche-like breakaway to the condensed phase. Although we are not inclined to consider the instability that we obtained on an ideal crystalline surface as the only reason for the high activity of a silver iodide aerosol as a stimulator of nucleation (the instability enters into the picture only at extremely high values of the supersaturation), the behavior of the system after the appearance of the instability is interesting in its own right as one of the factors contributing to the anomalously high activity of AgI. The crystalline structure of the AgI lattice itself gives its own positive contribution to the development of the instability. This is obvious even from the fact that, according to results of numerical experiments reported in my previous paper,[33] in the case of nucleation on individual Ag^+ and I^- ions outside the AgI lattice the instability is absent even at two times larger pressures ($P=50$ mbar). We were not able to observe the development of instability in nucleation on individual ions even over a wider range of conditions. Although the field of an individual ion, not screened by oppositely charged ions of the crystalline lattice, is much stronger than the field at the surface of the crystal, simply larger values of the stimulating field turn out to be insufficient for the development of the instability—the defining factor here turns out to be the field's structure.

Figure 5 (the curves marked *4*) displays the local density distribution above the Ag^+ and I^- ions after the development of the instability and the filling of the volume bounded by the hemisphere with radius $R=10$ Å above the surface of

the crystal. After the microvolume filled with water molecules, their number stabilized and fluctuated about its mean value $\langle N\rangle = 40.2$. In fact, the hemispherical space was introduced as a forced constraint on the growth of the number of particles in the system with the aim of not exceeding the calculational limits of the computer. We assume that the radius of the intermolecular correlations in the system is less than 10 Å so that the presence of an outer envelope bounding its growth does not have a decisive influence on the microstructure in the central part of the hemisphere, where the distributions presented in Fig. 5 are calculated—further growth of the microdroplet to macroscopic dimensions should not produce qualitative changes in the nature of the micromolecular interactions of the crystal surface with the microdroplet. If we accept this hypothesis, which to us seems eminently reasonable, then distributions *4* in Fig. 5 give a picture of the structure of the bulk dense phase at the boundary with the silver iodide crystal. We expect that these distributions accurately reflect at least the main trends and we will speak only of effects that can be measured in orders of magnitude.

The positions that are the most favorable for the water molecules on the surface of the crystal are those above the I^- ions at a height of 2.7 Å above the surface. The probability of finding a molecule at such a point is 100 times greater than above an Ag^+ ion (see Fig. 5). Obviously, the reason for such a selectivity is not the sign of the ion, but rather the fact that the Ag^+ ions are located in the first layer of the crystalline lattice while the I^- ions are located in the second. On the surface of the crystal there are formed natural "traps," consisting of three Ag^+ ions surrounding one I^- ion (see Fig. 3). The water molecules which fall into these "traps" serves as links, after a fashion, connecting the crystal surface with the dense phase of H_2O.

The development of the instability is accompanied by an abrupt falloff of the interaction energy for the I^- ions from the positive value $+0.25$ eV$\approx 11kT$ to the negative value -0.08 eV$\approx -3.5kT$ (see Fig. 6). Conversely, the interaction energy for the Ag^+ ions grows by roughly the same amount from -0.46 eV to -0.13 eV. The resulting binding energy with the surface per molecule remains unchanged; however, it is necessary to take into account that in the nascent system some of the molecules were in additional monomolecular layers above the surface and had almost no direct interaction with it, while the energy plotted in Fig. 6 is the result of averaging over all the molecules of the system, so the molecules of the first monomolecular layer were more strongly bound to the surface than before the onset of the instability (curves *1–3* in Fig. 5). In addition, the surface density of the molecules in the first layer increased by more than three orders of magnitude. As a consequence, the surface density of the binding energy of a molecule with the crystal after the development of the instability grew by almost four orders of magnitude. Changing the sign of the interaction of the molecules with the I^- ions means reorienting the dipole moments of a significant fraction of the molecules by 180°. Obviously, such a rotation was induced by the molecules of the second monomolecular layer. This confirms the idea that the main obstacle on the path of growth of the dense phase on the surface of the crystal is the unfavorable orientational order in the first monomolecular layer in the initial stage of adsorption. It is interesting that a break in this order by the molecules of the subsequent layers does not decrease the binding energy of the first layer with the surface, but rather makes this binding (or adhesion) stronger. Obviously, a lower energy corresponds to a new induced orientational order in the first layer, but a simultaneously lower entropy—in other terms, to deeper, but narrower local minima in the energy surface.

The interaction between the molecules after the development of the instability is increased by two orders of magnitude and is equal to $u_v = -0.28$ eV$\approx -13kT$, and the interaction with the crystal is equal to $u_s = -0.20$ eV per molecule (see Fig. 6). If a microdroplet were to grow by a simple increase of all its linear dimensions without any change in shape, then the contribution from the interaction with the surface u_s would decrease relative to the volume term u_v, and the total energy of the system per molecule would increase, asymptotically approaching u_v, which is thermodynamically unfavored. Therefore the microdroplet will grow while simultaneously "sprawling" across the surface of the crystal. In a system of 40.2 molecules this tendency is already quite pronounced: at distances of up to 5 Å from the surface of the crystal a microstructure is clearly visible in the density distribution that is connected with the microcrystalline structure of the surface itself. In the next 5 Å above the surface, microscopic inhomogeneities in the distribution smooth out and the density decreases smoothly by roughly a factor of three as one moves out to 10 Å above the crystal. Here the shape of the nucleus is more flat than spheroidal and with removal of the limiting hemisphere will grow more quickly along the surface than out from it. For a final answer to this question, it is necessary to carry out numerical experiments with a large number of particles.

The bulk density averaged over the volume of the hemisphere is 0.019 $Å^{-3}$ or 60% of the density of water under normal conditions. In the layer between 2 Å and 4 Å above the surface of the crystal, i.e., in the region of the first molecular layer, the mean bulk density is close to the density of water (ice). To assign a specific aggregate state (liquid water, ice) to such a system would be, strictly speaking, incorrect by virtue of its extreme inhomogeneity and microscopic size. According to rigorous statistical theory,[16] phase transitions in the strict sense as singular points of thermodynamic potentials take place only in the thermodynamic limit $N\to\infty$. In a finite, bounded molecular system one observes only the more or less pronounced traces of these transitions.[17-31] In terms of its density, the character of its correlation functions, and its weakly expressed long-range order, the adsorbed phase observed in our numerical experiment is closest to a liquid.

We carried out a series of numerical experiments with strong supersaturation which reproduced the avalanche-like growth of the nucleus in the nonstationary segment of the Markov process as a result of fluctuational growth of the number of molecules in the system. For the instability to develop at vapor pressures $P > 30$ mbar, a fluctuation with an amplitude less than 5–7 molecules in the system is suffi-

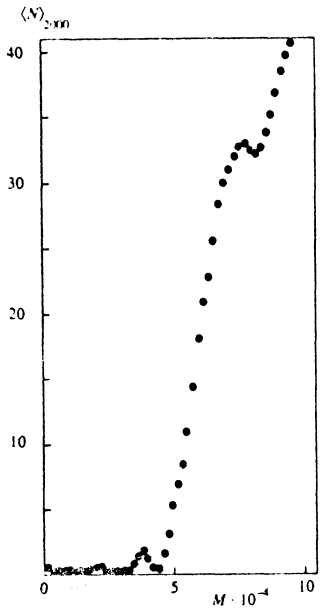

FIG. 8. Example of onset of avalanche-like growth of the nucleus of dense-phase water on the surface of an ideal β-AgI crystal in the presence of strong supersaturation ($P=81$ mbar) in the nonstationary segment of the Markov process at $T=253$ K. The vertical axis plots the partial mean number of molecules in the system, averaged over $2\cdot 10^3$ Markov steps; the horizontal axis plots the number of Markov steps taken.

cient. This quantity should be considered as an upper estimate on the size of a critical nucleus. An example of the development of such an instability is shown in Fig. 8. In the first $5\cdot 10^4$ Markov steps the number of particles in the system oscillates stably in the region of one molecule, then it suddenly breaks away to large values. Such a behavior of the system speaks of the presence of a thermodynamic barrier corresponding to a critical size.

Recall that, strictly speaking, the Markov process proposed by Metropolis[39,40] and realized in the present work does not reproduce the evolution of the system in real time[49]—here we are speaking only of calculating equilibrium mean values, and the order of summation of the current values is violated here. The Markov step counter (horizontal axis in Fig. 8) does not correspond to physical time; however, the specific character of the development of the instability in Markov "time" indicates the presence of a thermodynamic barrier retarding the growth of the nucleus. Determining the exact position of this barrier in the space of dimensions of the cluster is not one of the tasks of the present work. For us it is important to establish the factors in the structure of the crystalline lattice of sodium iodide that are capable of having a radical effect on the critical size and on the profile of the dependence of the work of formation of a microdroplet on it size. The results of this study allow us to assert with confidence that under nucleation conditions on the surface of an ideal crystal of silver iodide there exists a thermodynamic barrier to the growth of a nucleus, as in the case of homogeneous nucleation in a gas, which should be interpreted as a critical size. Overcoming this barrier as a result of density fluctuations in the system is possible only when the critical size becomes comparable with the amplitude of these fluctuations. Such conditions on the surface of an ideal crystal are reached only at very high supersaturation levels (by a factor of between one and two orders of magnitude) and are not capable of explaining the high activity of silver iodide aerosol observed in the field at much lower supersaturation levels. Thus, the "successful" hexagonal structure of an ideal crystal of silver iodide is not by itself the only reason for the high adsorptive power of silver iodide aerosol toward water, although it introduces its own positive contribution against the background of other stimulating factors. A consistent approach to the solution of this problem would require that we turn our attention to the role of crystalline defects.

The main question that we are trying to answer is, first, do crystalline defects promote the thermodynamic instability of a nucleus on the surface of the crystal, leading to its growth up to macroscopic dimensions? We begin our study with the simplest point defects of vacancy type. The creation of such a defect reduces to removing one ion from the crystalline lattice. The local microdeformation of the lattice associated with changing the position of the ions neighboring the vacancy is a higher order effect relative to the strong electric field in the region of the vacancy due to the local violation of electrical neutrality, and we do not take it into account. Figure 9 depicts the evolution of the number of particles in the system at the first 10^5 Markov steps in the case of a vacancy defect at the position of an I^- ion. Such behavior was reproduced in a series of numerical experiments. Figure 9 is a typical example. Water molecules are drawn into the electric field of the defect accumulate around it. Over the first $(5-7)\cdot 10^4$ steps of the nonstationary Markov process stable growth of the size of the molecular cluster is observed up to saturation. Saturation is followed by fluctuations about this saturation size, indicating the attainment of equilibrium. The molecules fill up roughly 1/5 of the volume around the defect under the limiting hemisphere above the surface of the crystal. Strictly speaking, this equilibrium state is locally stable since at fixed temperature and pressure the absolutely stable phase is the bulk solid phase—ice. Long-lived metastable states arise if the amplitude of the natural fluctuations in the system are much less than is needed to lead the system out of equilibrium, i.e., if the local minimum of the free energy corresponding to this local stable state has a width significantly exceeding the amplitude of the fluctuations in the system. It is just such a situation that we are dealing with here in the case of nucleation in the field of a point crystalline defect—a locally stable molecular cluster is formed just like in the case of nucleation on isolated ions.[33] The temperature and pressure of the vapor over wide ranges does not take such a cluster out of equilibrium, although its equilibrium size varies somewhat.

The reason for the slowing down of the growth of the cluster in the field of a point defect must be sought in its microstructure. The local density in the nucleus falls off rapidly with distance from the center of the defect. Whereas the density reaches its maximum at a height of 3.3 Å above the Ag^+ ions in the nearest coordination layer at a distance of 2.5 Å from the center, with a value close to the bulk density in the liquid phase (Fig. 10), at a distance of 5 Å above the

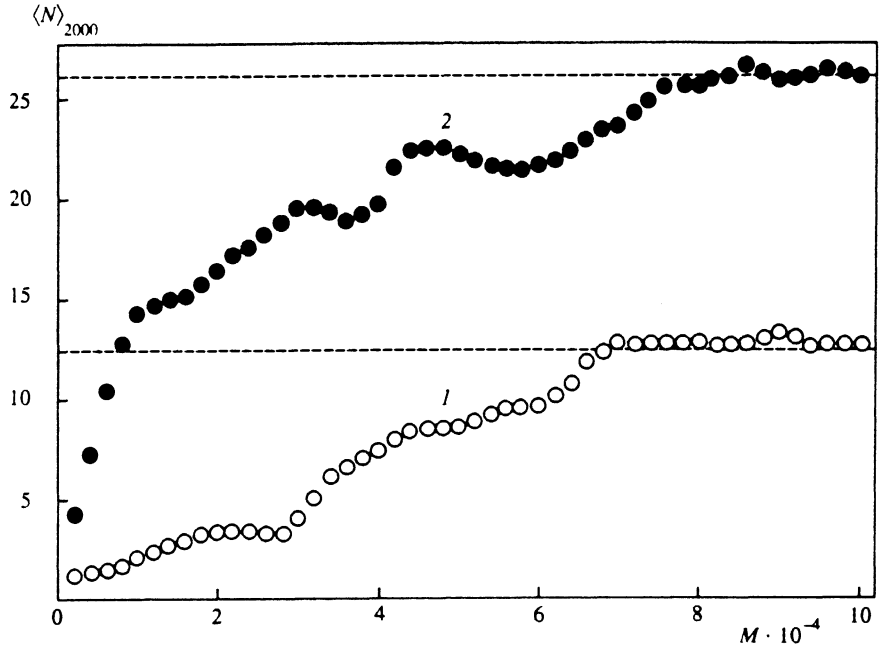

FIG. 9. Evolution of the partial mean size of the nucleus formed in the field of a point defect on a base face of a β-AgI crystal, in the nonstationary segment of the Markov process at $T=253$ K and $P=1$ mbar. The dashed line shows the mean number of molecules after $1.2\cdot 10^6$ additional Markov steps. Key to curves: *1*—in the field of a vacancy-type defect at the position of an I^- ion, *2*—in the field of a replacement-type defect where a Ag^+ ion has been replaced by an I^- ion.

Ag^+ ions in the second coordination layer the density decreases by roughly a factor of 25. The molecular cluster has, on average, a shape close to spherical with a radius of about 4.5 Å. The molecules are located mainly near the I^- ions in the first coordination layer around the defect at a distance of 4.5 Å from the vacancy (Fig. 10). Although the sign of the electric field of the defect corresponds to local violation of electrical neutrality in favor of positive charge, the maximum local density is reached not above the Ag^+ ions, but above

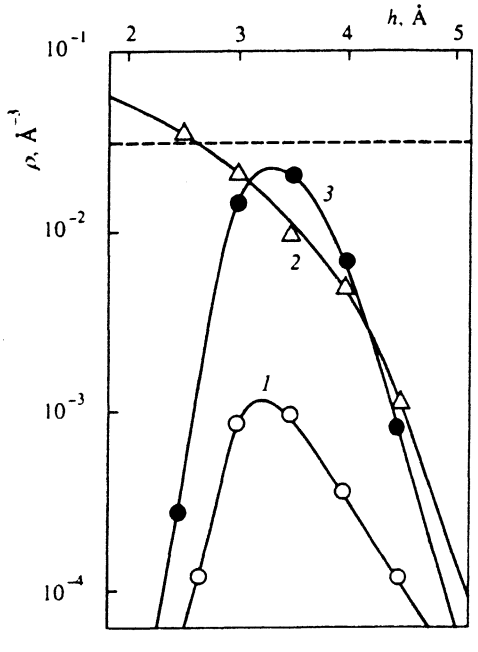

FIG. 10. Local density distributions in a dense-phase water nucleus forming in the field of a point vacancy defect at an I^- position, versus height above the crystal surface at $T=253$ K and $P=1$ mbar: *1*—above Ag^+ ions in the second coordination layer around a vacancy, *2*—above I^- ions in the first coordination layer around a vacancy, *3*—above Ag^+ ions in the first coordination layer. Dashed line—bulk water density under normal conditions.

the I^- ions—in the natural cells between the silver ions on the surface of the crystal. The interaction with the Ag^+ ions is attractive and is equal to -0.59 eV$=-27kT$ per unit molecule. The interaction with the I^- ions is of a loosening nature and is equal to $+0.12$ eV$=+5.4kT$. The sign of the interaction energy implies that the orientation of the dipole moments of the molecules imposed by the field of the positive silver ions is favored. Here the favored position of the molecules is above the iodide ions. The binding interaction between the molecules of the nucleus is equal to -0.14 eV$=-6kT$, equal to 30% of the interaction energy with the surface of the crystal. The stability of the cluster is ensured to a significant extent by direct interaction with the field of the crystalline defect; collective effects inside the nucleus are weakly developed and not capable of ensuring its growth. Growth of the nucleus at $P=1$ mbar stops at $\langle N\rangle=12.3$ molecules. Supersaturation of the vapor by a factor of several does not violate the stability of the nucleus, and only increases its size by 30–50%, depending on the degree of supersaturation. The reason for stabilization of the size of the nucleus and slowing down of its growth is the very strong, and at the same time narrowly localized, electric field of the point defect. In the immediate vicinity of the defect the microstructure of the nucleus is crushed by the strong electric field. At distances greater than 5 Å the field of the defect is not strong enough to keep the molecule in the cluster. At the same time, the microstructure of the cluster at these distances is not able to readjust itself and become independently stable. It is specifically at these intermediate distances that the most unfavorable conditions for growth of the nucleus are realized—a thermodynamic barrier to nucleation arises. Delocalization of the electric field with simultaneous decrease of its magnitude should facilitate the lowering of this barrier. Such an electric field configuration can be obtained from a set of crystalline defects located at deeper lay-

ers of the crystalline lattice, or as a result of electrically charging the aerosol. Electrical charging can be the result of intense mechanical and thermal processing of the aerosol in a torch flame and can also arise as a result of the external photoelectric effect. The excess charge in the form of delocalized electrons will be distributed in this case in accordance with the general principles of electrostatics, i.e., preferentially on the surface of the aerosol particle. The thermal De Broglie wavelength of the thermalized electrons may serve as an upper estimate of the degree of quantum-mechanical delocalization of the charge. At $T=253$ K this wavelength is equal to 40 Å. However, the observed degree of localization can be higher due to statistical fluctuations of the electronic component and a difference of two orders of magnitude in the time scales of the electronic and molecular subsystems.

The regime of nucleus formation at a point defect does not undergo any qualitative changes in shifting from a vacancy at the position of an I^- ion to a vacancy at the position of an Ag^+ ion. The size of a stable nucleus at the same pressure and temperature increases to $\langle N\rangle=17.0$ molecules, the interaction with the negative iodide ions changes sign and acquires a binding character with energy -0.45 eV$=-21kT$ per molecule. The interaction with the positive silver ions acquires a loosening character, but is weak: $+0.03$ eV$=+1.4kT$. The internal intermolecular interactions in the nucleus are increased by a factor of 1.5 in comparison with the previous case and reach -0.21 eV$=-10kT$ per molecule, which is 50% of the interaction energy with the surface of the crystal. These results imply that conditions of nucleus formation in the field of a vacancy in the position formerly occupied by an Ag^+ ion in the first crystalline layer is more favorable than with a vacancy in the position formerly ccupied by an I^- ion in the second layer; however, fundamentally the situation has not changed, and the nucleus stops growing even for multiply supersaturated vapor. The spatial structure of the microcluster is extremely irregular. The local density above the geometric center of the vacancy defect is an order of magnitude smaller than above the ions in the nearest neighboring coordination layers (Fig. 1). In spite of the average loosening nature of the interaction of the microdroplet with the positive silver ions, the nucleus advanced the furthest of all in its growth above the surface above the Ag^+ ions. At a height of 5 Å above the surface the local density above the Ag^+ ions of the first coordination layer around the geometric center of the defect is on the order of the bulk density of liquid water under normal conditions, while above the neighboring negative iodide ions it is two orders of magnitude less (Fig. 11). For comparison, note that in the absence of a defect and for moderate supersaturation levels the values of the local density above the I^- and Ag^+ ions equalize at this height and are five orders smaller (cf. Fig. 5). The highest density is reached above the I^- ions at heights of 2.5–3.0 Å above the surface, and as one moves to ionic layers more distant from the center of the defect the density falls off monotonically at heights greater than 3 Å. At small heights it behaves extremely irregularly, which testifies to the complex structure of the first monomolecular layer. The highest density is

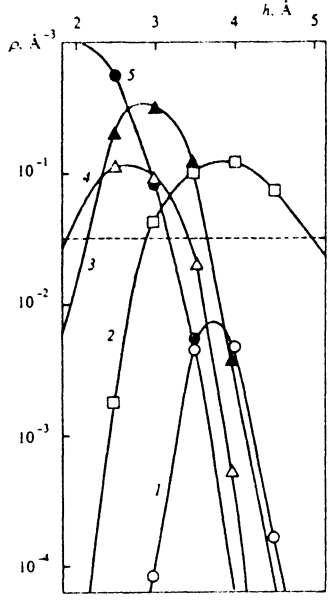

FIG. 11. The same as Fig. 10, but for vacancy defects at a Ag^+ position: *1*—above a vacancy at a Ag^+ position, *2*—above Ag^+ ions in the first coordination layer around such a vacancy, *3*—above I^- ions in the first coordination layer, *4*—above I^- ions in the second coordination layer, *5*—above I^- ions in the third coordination layer.

reached above the ions in the third coordination layer of I^- ions (7 Å from the center of the defect) at a height of 2–2.5 Å above the surface (Fig. 11) in a way that is similar to how this takes place in the independently stable dense adsorbed phase above an ideal crystalline surface in the presence of strong supersaturation (Fig. 5). At heights less than 2.2 Å above the surface the density above the first (3 Å from the center of the defect), second (5 Å), and third (7 Å) coordination layers of I^- ions, does not decrease as one moves away from the center of the defect as it does at larger heights, but, on the contrary, increases. This confirms our earlier conclusion that a strong electric field in the central part of the defect has a depressing effect on the stability of the nucleus.

The strongest and most concentrated source of an electric field on the surface of a crystal is a replacement defect. Modeling such a defect reduces to replacing one of the ions of the lattice by its opposite. Figures 9 and 12 display the results of modeling nucleation in the field of a replacement defect obtained by replacing an Ag^+ ion in the first crystalline layer by an I^- ion. The defect field, stronger than in the case of a vacancy, did not destabilize the nucleus. Growth of the nucleus at $P=1$ mbar reaches its saturation $\langle N\rangle=26.3$ molecules irrespective of the initial number of particles in the system (Fig. 9). The approach to the equilibrium size takes place during the first $(5-7)\cdot 10^4$ Markov steps. The size of the nucleus is no greater than its size in a vacancy defect field—the molecular cluster becomes denser in its central part. Shifting from a vacancy defect to a replacement defect involves an increase by a factor of 20 in the density above the geometric center of the defect (see Figs. 11 and 12). The height of the upper boundary of the nucleus above the surface decreased by roughly 1 Å while its trans-

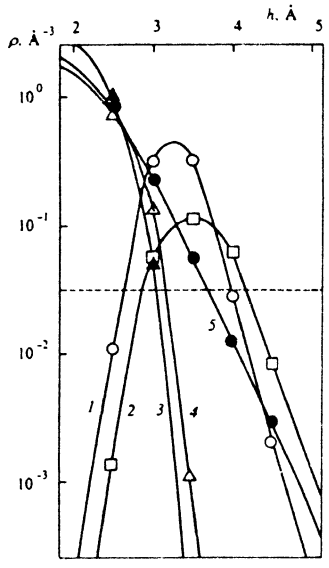

FIG. 12. The same as Fig. 10, but for a replacement defect where a Ag^+ ion has been replaced by an I^- ion: *1*—above the replacing I^- ion, *2*—above Ag^+ ions in the first coordination layer, *3*—above I^- ions in the first coordination layer, *4*—above I^- ions in the second coordination layer, *5*—above I^- ions in the third coordination layer.

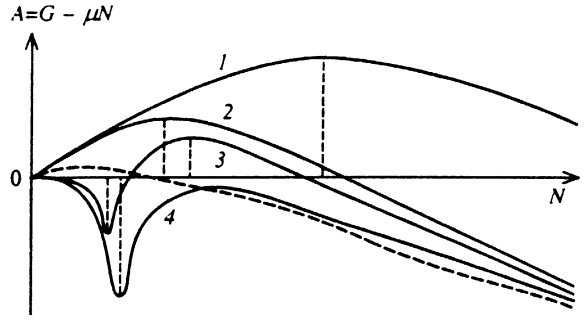

FIG. 13. Profiles of the dependence of the work function of dense-phase water nucleus formation under various conditions (schematically): *1*—in a homogeneous vapor without admixtures, *2*—on the surface of an ideal crystalline lattice, *3*—in the field of a vacancy-type point-defect on the surface of the crystal, *4*—in a strong defect field, where the defect is replacement by an oppositely charged ion. Dashed line—presumed dependence of the work function for nucleation on the surface of a crystal in the electric field of the optimal configuration.

verse dimensions increased by roughly the same amount, i.e., the cluster flattened. The height of the molecular clot above the surface of the crystal decreased due to destruction of the second monomolecular layer, the basis of which in the case of a vacancy defect (Fig. 11) is the molecules above the Ag^+ ions. The strong electric field of the extra I^- ion imposes an orientation on the molecular dipole moments that corresponds to repulsion from the Ag^+ ions and destruction of the weak second monomolecular layer.

The destabilizing action of the strong, nonuniform electric field in the case of a replacement defect is more pronounced and extends to greater distances. For this reason, in contradistinction to the case of a vacancy defect, in the field of a replacement defect the density of the nucleus at heights >2.5 Å increases with distance from the replacement ion I^- (Fig. 12). The nonuniformity increases with height above the surface of the crystal, and at a distance of 4.5 Å from the surface the density of the nucleus above the third coordination layer (7 Å from the center of the defect) exceeds the density above the first (3 Å) and second (5 Å) layers by not less than three orders of magnitude (Fig. 12).

The interaction energy of the molecules with the iodide ions, as determined by the model calculation, is negative and equal to -0.69 eV$=-32kT$ per molecule, and with the silver ions is positive and equal to $+0.15$ eV$=7kT$. The interaction energy between the molecules of the cluster, again as determined by the model calculation, is negative and equal to -0.17 eV$=-8kT$ or 31% of the binding energy with the crystal surface.

5. CONCLUSION

The Monte Carlo method allows one to directly calculate the free energy of a molecular system and the work of forming a nucleus from the gaseous phase, however, obtaining this information requires the expense of additional computational resources and is a problem of independent interest in its own right.[29–31] On the basis of the results already available we can put together a definite picture of the behavior of the free energy of a nucleus on the surface of a crystal of silver iodide, which is depicted schematically in Fig. 13. Curve *1* represents the work of forming a microdroplet from a homogeneous vapor in the absence of nucleation centers. The position of the maximum corresponds to the critical dimension. Supersaturated (metastable) states of the vapor arise as a consequence of the vanishingly small probability of fluctuational formation in the gas of a nucleus of greater than critical size. The critical size decreases with increasing supersaturation. Curve *2* represents the work of forming a nucleus on the surface of an ideal crystal, at the same temperature and pressure of the vapor. The work of formation in this case is lower as a consequence of the stimulating role of the crystalline surface, and the critical size is less; however, it remains high enough that the critical nucleus can form as a result of random fluctuations within times realizable in real experiments. Only in the presence of strong supersaturation (a factor of between one and two orders of magnitude relative to saturation) does the critical size drop down to a magnitude reachable via fluctuations—an instability develops with avalanche-like growth of the nucleus all the way to macroscopic dimensions ($N\to\infty$) and simultaneous lowering of the free energy. The instability is due to the negative work $\partial A/\partial N<0$ of joining new molecules for N greater than its critical value (Fig. 13).

The picture changes qualitatively after introducing a vacancy point defect on the surface of the crystalline substrate. In the region of the vacancy the balance between positive and negative ions is violated—a point source of a strong electric field is created. Water molecules are drawn into the region of the vacancy; however, the nascent molecular cluster has a microstructure far from that of the stable bulk phase of water. With increasing distance from the point defect, the

binding action of its field falls off faster than the microstructure of the nucleus is able to change from a microstructure imposed by the strong electric field of the defect to an independently stable microstructure, similar to the structure of ice. Growth of the cluster becomes thermodynamically unfavored and stops. Such a microcluster on the surface of the crystal is locally thermodynamically stable and corresponds to a local minimum in the work of formation (Fig. 13, curve *3*). The defect field lowers the work of formation somewhat (cf. curves *2* and *3*), but the critical size (position of the maximum in curve *3*) cannot decrease—on the contrary it increases. A possible physical reason for the increase of the critical size consists in distortions introduced by the electric field of the defect to the structure of the inner region of the nucleus. Thus, the introduction of a point defect in the crystal surface does not annihilate the critical barrier on the path of growth of the nucleus, but stable clusters of water molecules are formed around the defects. Even strong levels of supersaturation, all the way up to 10^2 do not convert these clusters into sources of instability, and the adsorptive power of the crystal remains low. The introduction into the structure of the crystal of more powerful electric field sources without altering their point character, e.g., defects in which an ion is replaced by an ion of opposite sign, does not qualitatively change the picture. Although the minimum in the dependence of the work of formation on the size of the nucleus becomes deeper, the barrier to growth of the nucleus in the form of a maximum in the same dependence remains high (Fig. 13, curve *4*). Even if the curve of the work function to the right of the minimum is located below the level $A=0$ (curve *4*), i.e., formation from the vapor of a microdroplet larger than the stable size is accompanied by a lowering of the free energy, this does not mean that such a process is actually realized within the observation time of a real experiment. Strictly speaking, a thermodynamic state with a lower free energy is realized in thermodynamic equilibrium, i.e., in the limit of an infinite expectation time $t\to\infty$. In reality there exists a rigid temporal hierarchy of the various paths of evolution of the system. At times realizable in a physical experiment the most probable path is realized, being the successive joining of molecules to an already-formed molecular cluster, i.e., continuous movement from left to right along the axis of size of the nucleus N in Fig. 13. Regions in which, the sign of the work of joining a molecule to the already-formed nucleus, is positive $\partial A/\partial N$, present a barrier on this path irrespective of the sign of the work of formation A.

The reason for the low effectiveness of the types of defects considered is their point character. The field of such defects is too strong, and the optimal microstructure of the nucleus is broken. On the other hand, the stimulating action of the field of such defects is strongly bounded in space and breaks off, in our opinion, too abruptly. A more favorable action on the critical size, from the point of view of nucleation, would be provided by a more uniform and weaker electric field, whose action would extend over regions with dimensions of the order of the geometric dimensions of a critical nucleus and beyond. Such a field could be created by the optimal arrangement of a set of point defects inside the crystal, and by breaks and fissures in the crystalline structure. The dashed curve in Fig. 13 depicts the conjectured dependence of the work of formation on the size of the nucleus in the field of defects of such type. We regard the form of this dependence as a very likely hypothesis.

ACKNOWLEDGMENTS

This work was carried out with the financial support of the Russian Fund for Fundamental Research, Project No. 93-05-8181.

[1] B. J. Mason, *The Physics of Clouds* (Oxford, Clarendon Press, 1957).
[2] J. E. Mayer, J. Chem. Phys. **5**, 67 (1937); **18**, 1426 (1950); **19**, 1024 (1951).
[3] J. E. Mayer and P. G. Ackermann, J. Chem. Phys. **5**, 74 (1937).
[4] E. Salpeter, Ann. Phys. **5**, 183 (1958).
[5] H. L. Friedman, Mol. Phys. **2**, 23 (1959); **2**, 190 (1959).
[6] R. Abe, Progr. Theor. Phys. **22**, 213 (1959).
[7] N. P. Kovalenko and I. Z. Fisher, Usp. Fiz. Nauk **108**, 209 (1972) [Sov. Phys. Usp. **15**, 592 (1973)].
[8] M. Volmer and A. Weber, Z. Phys. Chem. **119**, 227 (1926).
[9] L. Farkas, Z. Phys. Chem. **A125**, 236 (1927).
[10] J. Frenkel, J. Chem. Phys. **7**, 200 (1939); **7**, 538 (1939).
[11] R. C. Tolman, J. Chem. Phys. **17**, 333 (1949).
[12] F. H. Stillinger, J. Chem. Phys. **38**, 1486 (1963).
[13] F. F. Abraham, J. K. Lee, and J. A. Barker, J. Chem. Phys. **60**, 246 (1974).
[14] C. Kittel, *Elementary Statistical Physics* (Wiley, New York, 1958).
[15] T. L. Hill, *Thermodynamics of Small Systems* (New York, 1963).
[16] T. L. Hill, *Statistical Mechanics: Principles and Selected Applications* (McGraw-Hill, New York, 1956).
[17] C. L. Briant and J. J. Burton, Nature **243**, 100 (1973); J. Chem. Phys. **63**, 2045 (1975).
[18] J. K. Lee, J. A. Barker, and F. F. Abraham, J. Chem. Phys. **58**, 3166 (1973).
[19] W. D. Kristensen, E. J. Jensen, and R. M. J. Cotterill, J. Chem. Phys. **60**, 4161 (1974).
[20] R. D. Etters and J. Kaelberer, Phys. Rev. A **11**, 1068 (1975).
[21] J. Jellinek, T. L. Beck, and R. S. Berry, J. Chem. Phys. **84**, 2783 (1986).
[22] T. L. Beck and R. S. Berry, J. Chem. Phys. **88**, 3910 (1988).
[23] M. Bishop and C. A. Croxton, J. Chem. Phys. **90**, 1212 (1989).
[24] H. T. Diep and S. Sawada, Phys. Rev. B **39**, 9252 (1989).
[25] P. N. Vorontsov-Vel'yaminov and V. A. Pavlov, Teplofiz. Vys. Temp. **13**, 302 (1975).
[26] V. A. Pavlov and P. N. Vorontsov-Vel'yaminov, Teplofiz. Vys. Temp. **15**, 1165 (1977).
[27] P. N. Vorontsov-Vel'yaminov and S. V. Shevkunov, Fiz. Plazmy **4**, 1354 (1978) [Sov. J. Plasma Phys. **4**, 756 (1978)].
[28] S. V. Shevkunov and P. N. Vorontsov-Vel'yaminov, Teplofiz. Vys. Temp. **20**, 1025 (1982); Khim. Fiz. **1**, 83 (1983).
[29] S. V. Shevkunov, A. A. Martsinovski, and P. N. Vorontsov-Vel'yaminov, Teplofiz. Vys. Temp. **25**, 246 (1988).
[30] S. V. Shevkunov, A. A. Martsinovski, and P. N. Vorontsov-Vel'yaminov, Molecular Simulation **5**, 119 (1990).
[31] A. A. Martsinovski, S. V. Shevkunov, and P. N. Vorontsov-Vel'yaminov, Molecular Simulation **6**, 143 (1991).
[32] P. Buffat and J. P. Borel, Phys. Rev. A **13**, 2287 (1976).
[33] S. V. Shevkunov, Zh. Éksp. Teor. Fiz. **105**, 1258 (1994) [JETP **78**, 677 (1994)].
[34] S. V. Shevkunov and A. A. Al'mukhrez, Khim. Fiz. **13**, No. 11, 117 (1994).
[35] A. Rahman and F. H. Stillinger, J. Chem. Phys. **55**, 3336 (1971); J. Am. Chem. Soc. **95**, 7943 (1973).

[36] F. H. Stillinger and A. Rahman, J. Chem. Phys. **57**, 1281 (1972); **60**, 1545 (1974); **61**, 4973 (1974).
[37] F. H. Stillinger, Adv. Chem. Phys. **31**, 2 (1975).
[38] B. H. Hale and J. Kiefer, J. Chem. Phys. **73**, 923 (1980).
[39] N. Metropolis, A. W. Rosenbluth, M. N. Rosenbluth, and H. A. Teller, J. Chem. Phys. **21**, 1087 (1953).
[40] M. N. Rosenbluth and A. W. Rosenbluth, J. Chem. Phys. **22**, 881 (1954).
[41] B. J. Alder and T. E. Wainwright, J. Chem. Phys. **31**, 459 (1959).
[42] P. Turq, F. Laatelme, and H. L. Friedman, J. Chem. Phys. **66**, 3039 (1977).
[43] P. Turq and F. Laatelme, Molec. Phys. **37**, 223 (1979).
[44] D. L. Ermak, J. Chem. Phys. **62**, 4189 (1975); **62**, 4197 (1975).
[45] H. A. Ceccatto, Phys. Rev. B **33**, 4734 (1986).
[46] H. C. Kang and W. H. Weinberg, J. Chem. Phys. **90**, 2824 (1989).
[47] J. R. Ray, M. C. Moody, and A. Rahman, Phys. Rev. B **33**, 895 (1986).
[48] A. P. Lyubartsev, A. A. Martsinovski, S. V. Shevkunov, and P. N. Vorontsov-Velyaminov, J. Chem. Phys. **96**, 1776 (1992).
[49] V. M. Zamalin, G. E. Norman, and V. S. Filinov, *The Monte Carlo Method in Statistical Thermodynamics* [in Russian] (Nauka, Moscow, 1977).
[50] G. Burley, Am. Mineralogist **48**, 1266 (1963); J. Phys. Chem. Solids **55**, 629 (1964).
[51] W. Buhrer and R. M. Nicklow, Phys. Rev. B **17**, 3362 (1978).
[52] *Chemistry Handbook* [in Russian] (Khimiya, Leningrad, 1971), p. 404.
[53] R. W. G. Wyckoff, *Crystal Structures* (Interscience Publishers, New York, 1965), p. 110.
[54] P. P. Evald, Ann. Phys. **21**, 1087 (1921).
[55] I. S. Grigor'eva and E. Z. Meĭlikhova, eds., *Physical Quantities* [in Russian] (Energoatomizdat, Moscow, 1991), p. 254.

Translated by Paul F. Schippnick